Greenhouse Gas Emissions from Agricultural Land Before and After Permanent Flooding with Seawater or Freshwater

Susan Guldberg G. Petersen[1] · Erik Kristensen[1] · Cintia O. Quintana[1]

Abstract

Sea level rise driven by global warming is threatening low-lying and reclaimed agricultural areas near coasts. The most marginalized of these with low crop yield can be converted into new valuable wetland ecosystems with high CO_2 mitigation capacity by removing drainage systems or performing managed realignment. This study assessed CO_2 and CH_4 dynamics before and after forming two adjacent wetlands by flooding reclaimed agricultural land. The Gyldensteen Coastal Lagoon (214 ha) is an open system flooded with seawater, and the neighboring Lake Engsø (144 ha) is a closed system flooded with freshwater. Before flooding in 2014, the total area was a net source of about 10,350 Mg CO_2 yr^{-1} due to aerobic microbial soil respiration. The temporal and spatial pattern of CO_2 and CH_4 release changed after flooding in a pattern that depended on soil biogeochemistry, temperature, and other environmental factors. Thus, there were strong exponential temperature dependencies of CO_2 and CH_4 emissions. Slow anaerobic microbial action in the Coastal Lagoon soil and the presence of sulfate prevented CO_2 and CH_4 emission, leading to a slight net uptake of CO_2 in 2019 (-70 Mg CO_2 yr^{-1}). Conversely, methanogenesis near the soil–water interface after freshwater flooding of Lake Engsø drove rapid emission of CH_4 (diffusive and ebullitive) that doubled its greenhouse gas emissions. In conclusion, CH_4 emissions in Lake Engsø therefore counteracted the CO_2 mitigation effect by flooding and the total area remains a net source of greenhouse gases with an emission of 8330 CO_2-equivalents yr^{-1}.

Keywords Restored wetlands · CO_2 emission · CH_4 emission · Flooding · Seawater · Freshwater

Introduction

Climate change has increased the risk of coastal flooding worldwide due to sea level rise combined with more extreme weather (such as storm surges). According to the Intergovernmental Panel on Climate Change (IPCC), the rate of sea level rise today is 3–6 times faster than the average of the last 100 years and is projected to increase further (Oppenheimer et al. 2019). This will pose a challenge in low-lying countries such as Denmark, where large coastal areas are in danger of being flooded. The most effective solution to this problem is to dampen the warming by a significant global reduction in greenhouse gas (GHG) emissions. However, since it is unlikely that the needed reduction goals will be reached, climate adaptation is required. An obvious climate adaptation strategy in low-lying coastal areas of inferior economic value is "managed realignment," where old coastal defenses, such as dikes, are intentionally removed, and new are erected further inland (Andrews et al. 2006; Burden et al. 2013; Kristensen et al. 2021). As a result, new restored coastal wetlands of high ecological value are formed that can act as tidal buffer zones, protecting the hinterland against flooding and simultaneously preventing loss of essential infrastructure.

Coastal wetlands have increasingly been recognized as important climate mitigation habitats due to their protective ability (Gedan et al. 2011) and capacity for sequestering carbon in the wet and anoxic soils (Chmura et al. 2003; Mitsch et al. 2013; Kroeger et al. 2017). Despite occupying only 5–8% of land-habitat areas, it has been estimated that around 20–30% of the Earth's upper 2 m soil pool of 2500 Pg carbon is stored in these wetlands (Lal 2008; Davidson 2014). Unfortunately, wetlands have disappeared at an alarming rate of more than 50% over the last century (Li et al. 2018), and

✉ Susan Guldberg G. Petersen
  guldberg.susan@gmail.com

1   Department of Biology, University of Southern Denmark, Campusvej 55, 5230 Odense M, Denmark

along with them, their capability as GHG-mitigation habitats, physical buffer zones, and other ecosystem services.

Several freshwater and marine wetlands have in recent years been restored (Hartvigsen 2014; Chimner et al. 2017; Cadier et al. 2020). In Denmark, large areas of agricultural land have been marginalized for decades providing crop yields which are no longer profitable (Stenak 2005). Many of these are reclaimed land and are as such old marine or freshwater wetlands. Thus, about 45,000 ha farmland in Denmark is of marine origin (Nielsen et al. 2021). Such low-lying marginalized areas, and especially those with organic-rich soil, are ideal for wetland restoration by managed realignment and simultaneously function as a low cost and effective way for climate change mitigation (Crooks et al. 2011).

Carbon dioxide (CO_2) is the most important greenhouse gas that is generated in all ecosystems as a natural product of organic carbon degradation. It is released by all organisms ranging from metazoan consumers to microbial decomposers in oxic and anoxic environments (Canfield et al. 2005). More distressingly, large amounts of CO_2 are generated anthropogenically by combustion of fossil fuels. CO_2 has a global warming potential (GWP) of 1 regardless of the time period (Myhre et al. 2013). GWP of other gases indicates their ability to absorb heat in the atmosphere relative to CO_2 on a specific timescale. Methane (CH_4) is the second largest contributor to climate change after CO_2, not because of a large natural and anthropogenic production of CH_4, but rather due to its higher potential as greenhouse gas. CH_4 is, in contrast to CO_2, a "short-lived climate pollutant" that on average stays in the atmosphere for approximately 12 years before it is oxidized to CO_2 (Abernethy and Jackson 2022). Over a 100-year period, CH_4 is a 28–34 times more potent greenhouse gas than carbon dioxide. However, over a 20-year period, a yardstick that climate scientists have previously suggested as a more appropriate timeframe, CH_4 is up to 81 times more potent than CO_2 (Abernethy and Jackson 2022).

CO_2 is released in high amounts from oxic and nutrient-rich agricultural soils due to rapid aerobic bacterial respiration (Benbi 2013). When soils are (re)flooded and turn anoxic during construction of new wetlands, aerobic respiration is hampered and replaced by anaerobic respiration that is ~10 times slower, thus greatly reducing the CO_2 emission (Kristensen et al. 1995). However, freshwater and brackish wetlands can instead act as sources of CH_4 (Laanbroek 2010; Bastviken et al. 2011; Bridgham et al. 2013; Arias-Ortiz et al. 2021), thereby counteracting the mitigation gained by flooding. Formation of CH_4 occurs through methanogenesis, an obligatory anoxic process that is the ultimate step in carbon degradation. Whether a wetland acts as a GHG sink due to lowered CO_2 emission or a source due to excessive CH_4 emission depends on various physical, chemical, and

biological controls. These include the presence of sulfate, organic substrates, pools of inorganic and organic nutrients, type and presence of vegetation, hydrology, and temperature (Jørgensen 2006; Davidson et al. 2018; Pugh et al. 2018; Vroom et al. 2022). CH_4 is released from wetlands/lakes through different pathways, including diffusive, ebullitive, storage flux, and flux through aquatic vegetation (Sanches et al. 2019).

The objectives of this study were to quantify and compare emission of CO_2 and CH_4 from two newly formed Danish wetlands: a saline coastal lagoon and a freshwater lake. The study focuses on two key environmental conditions controlling emissions: (i) dry soil versus flooded soil and (ii) saltwater versus freshwater flooding. Effects of biogeochemistry and temperature will be assessed from surveys determining the spatial and temporal variation in emissions of these greenhouse gases. We hypothesize that (1) flooding decreases the microbial release of CO_2 from soils by turning oxic farmlands with rapid aerobic respiration into anoxic wetlands with slow anaerobic respiration; (2) soils flooded with seawater are dominated by sulfate reduction, while methanogenesis dominate soils flooded with freshwater leading to excessive release of CH_4; and (3) the temporal variation of CO_2 and CH_4 release depends primarily on temperature.

Materials and Methods

Study Area

The restored Gyldensteen Coastal Lagoon and the newly established Lake Engsø are located on northern Fyn near Bogense in Denmark (Fig. 1). Roughly 1000 ha of coastal seabed near Gyldensteen Manor was diked, drained, and cultivated in 1871 (Stenak 2005). After 140 years of agricultural activities, 615 ha of the land was acquired by the Aage V. Jensen Nature Foundation for nature restoration. This included the two new wetlands that were flooded in March 2014 after coastal reconstruction. Most of the area was used for barley and seed grass cultivation the years before flooding.

Gyldensteen Coastal Lagoon was established by managed realignment, where seaward dikes were partly removed, allowing seawater from Kattegat to flood the former agricultural land through 3 openings (Fig. 1). The restoration involved construction of new inland dikes to prevent excessive flooding. The Coastal Lagoon covers 214 ha with an average water depth of about 1 m. Average tidal amplitude is ~0.4 m, but with larger water fluctuations ($\pm$ 1 m) during periods of strong winds (Danish Meteorological Institute, DMI), providing less than 2-day residence time of water. Water temperature ranges from a winter low of ~0 °C to a
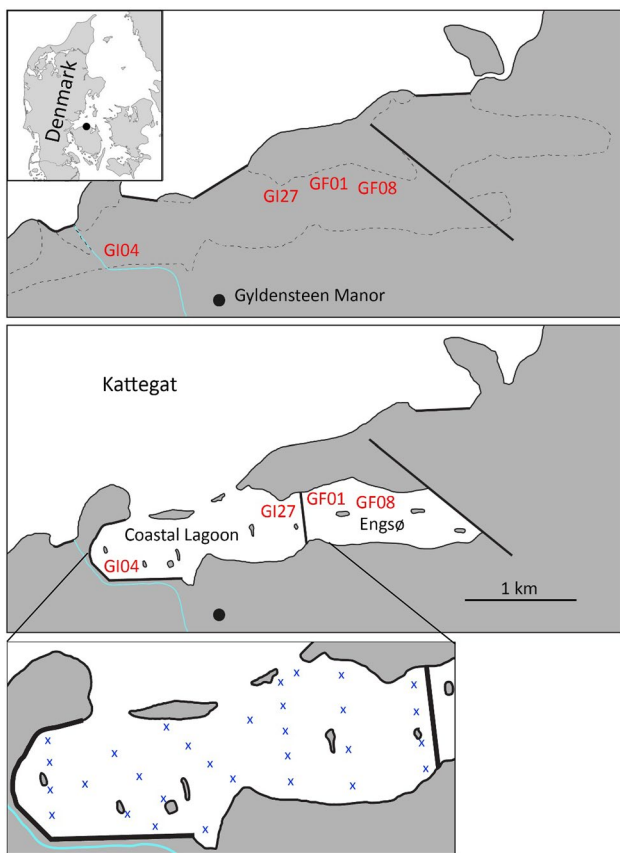
Fig. 1 Maps of the Gyldensteen area before (upper) and after (middle) managed realignment in 2014. The broken lines in the upper panel indicate the old coastline before land reclamation in 1871. Heavy lines in both panels indicate old and new dikes. The red codes represent the major measuring locations in the Coastal Lagoon and Lake Engsø. The 30 measuring stations (lower) visited before flooding are indicated with crosses in the zoom insert of the Coastal Lagoon. Station 1 is at northwest and station 30 is at southeast

summer high of ~20 °C, while salinity ranges between 20 and 25 all year round. There are no freshwater discharges to the system, except for few minor agricultural drainage channels in the southern part. The coastal lagoon today is mostly unvegetated but has scattered occurrence of brown

algae (*Fucus vesiculosus*) and red algae (*Gracilaria vermiculophylla*) (Thorsen et al. 2021). The major primary producers are therefore benthic diatoms and cyanobacteria. The marine area just outside the lagoon is shallow with water depths of 0.5–1 m and has scattered growth of *F. vesiculosus* several hundred meters offshore.

Lake Engsø is separated from the Coastal Lagoon by a dike, but otherwise located on soil with similar agricultural history (Fig. 1). It was formed passively after drainage of the farmland was terminated. The surrounding land (catchment area) is farmland, meadows, and forests. Since there are no freshwater inlets and outlets in the form of streams, water in Lake Engsø originates from precipitation, groundwater, and run-off from the adjacent fields. In case of overflow, water is led through a pipe to the Coastal Lagoon. Lake Engsø contained freshwater when it was established, but it is now slightly brackish with a salinity of 0.5–2 due to evaporation. It covers 144 ha with an average water depth of about 1 m. Water temperatures ranges from a winter low of ~0 °C to summer highs of up to 25 °C. Lake Engsø today is mostly unvegetated with some drifting plants and algae. The benthic flora is light limited due to high turbidity from massive phytoplankton growth.

CO_2 and CH_4 Flux Measurements

Soil-air, soil–water, and water–air fluxes of CO_2 and CH_4 were measured with variable spatial and temporal resolution in the Coastal Lagoon and Lake Engsø before and after flooding from 2013 to 2020 (Table 1).

Soil-Air CO_2 Emission in the Coastal Lagoon

In situ soil-air CO_2 emission from the agricultural soil prior to flooding was measured at 30 locations throughout the Coastal Lagoon area in September 2013. These were located primarily in areas vegetated with barley and seed grass and to a lesser extent in grassland. Seasonality and temperature dependence of soil-air CO_2 emission was determined on six occasions during 2014 (March, May, June, August,

Table 1 Overview of in situ and laboratory measurements in Gyldensteen Coastal Lagoon and Lake Engsø from 2013 to 2020

Year	Measurement	Note
2013	CO_2 soil-air fluxes (spatial)	In situ, Coastal Lagoon (before flooding)
2013–2014	CO_2 soil-air fluxes (temporal)	In situ, Coastal Lagoon (adjacent)
2015–2017	DIC fluxes soil–water	In situ, Coastal Lagoon
2018	CO_2 and CH_4 fluxes water–air	In situ, Coastal Lagoon and Lake Engsø
	DIC and CH_4 fluxes soil–water	In situ, Coastal Lagoon
	DIC and CH_4 fluxes soil–water	Laboratory, Lake Engsø
2019–2020	CO_2 and CH_4 fluxes water–air	In situ, Coastal Lagoon and Lake Engsø
	CH_4 ebullition water–air	In situ, Lake Engsø
	DIC fluxes soil–water	In situ, Coastal Lagoon
	DIC and CH_4 fluxes soil–water	Laboratory, Lake Engsø

September, and November) in moist soil of an adjacent pasture that was not flooded. A custom-made opaque 8 cm inner diameter and 10 cm high Plexiglas flux chamber was fitted gas tight to a Plexiglas collar of the same diameter that had been inserted 3 cm into the soil at least 30 min prior to measuring. Three replicate collars were at each measuring occasion placed on bare soil between the stubs of harvested barley and grass. The flux chamber was connected by a flow-through approach to a Li-Cor LI-6400 Portable Photosynthesis System that monitored CO_2 concentrations inside the chamber continuously every 10 s for 5 min. Three sequential measurements with ambient air flushing between were performed while the flux chamber remained fitted to each collar. Emission of CO_2 (mol m^{-2} d^{-1}) was calculated from the linear increase in concentration (M d^{-1}) and corrected for chamber volume (L) and area (m^2). Temperature was recorded by inserting an electronic soil thermometer 5 cm into the soil next to the collars.

Soil–Water DIC and CH_4 Exchange in the Coastal Lagoon

Seasonality and temperature dependence of in situ soil–water release of dissolved inorganic carbon (DIC) at the representative Coastal Lagoon station GI04 in the west and GI27 in the east (Fig. 1) was determined from measurements in winter (January–February), spring (May), summer (July–August), and fall (October) from 2015 to 2020. In addition, soil–water release of CH_4 was assessed at GI27 during all seasons in 2018. Six cylindrical flux chambers (40 cm i.d. and 20 cm deep) were deployed on unvegetated soil at each station 1 day before initiating the measurements. The transparent chambers were pushed about 5 cm into the soil and left with open tops overnight. The next day, all chambers were sealed, equipped individually with a stirrer motor driving a 5-cm long stirrer bar at about 60 rpm. Three chambers were covered by black plastic to prevent light intrusion and three were kept uncovered in light. Water samples for DIC and CH_4 analysis were taken through an otherwise sealed sampling port in the lid at the start and end of incubation. The incubation time was 3 to 5 h depending on season and the water temperature. The latter was measured with an electronic thermometer before and after incubations. Test showed that oxygen never decreased below 50% of saturation. Samples for DIC analysis (5 ml) were transferred to Exetainers, preserved with $HgCl_2$ and sealed gas tight. DIC was analyzed as soon as possible on a flow injection/diffusion cell analyzer (Hall and Aller 1992). Separate samples (10 ml) for CH_4 analysis in 2018 were preserved with $HgCl_2$ in gas tight Exetainers. In the laboratory, 2-ml sample was replaced with a headspace of N_2. The headspace gas was after equilibration analyzed for CH_4 at room temperature and atmospheric pressure by Gas Chromatography-Flame Ionization Detection (GC-FID). The flux of DIC and

CH_4 (mmol m^{-2} d^{-1}) was calculated from the difference in concentration from start to end (mM d^{-1}) and corrected for chamber volume (L) and area (m^{-2}).

Soil–Water Exchange of DIC and CH_4 in Lake Engsø

The soil–water exchange of DIC and CH_4 at station GF08 in the central deeper part of Lake Engsø was determined by core incubations under laboratory conditions. This was necessary because vegetation and high turbidity of the water prevented in situ incubations. Three cores (8 cm i.d. and 20 cm deep) of unvegetated soil were taken in winter (February) and summer (July) of 2019. The cores were carefully placed in tanks with water from Lake Engsø. They were left open with stirring (60 rpm) and oxygenation for minimum 48 h to acclimatize in a 12:12 h. Light/dark cycle (~400 µE m^{-2} s^{-1}) in a constant temperature room. Temperature was kept at 5 °C in winter and 15 °C in summer. Water samples for DIC and CH_4 analyses were taken before and after the cores were sealed with lids while maintaining stirring. Winter cores were incubated for 12–14 h while summer cores were incubated 4–5 h in the dark and light. Oxygen never dropped below 50% of saturation. Water samples were treated and analyzed, and results calculated as described above for in situ soil–water flux measurements in the Coastal Lagoon.

Water–Air Emission of CO_2 and CH_4 in the Coastal Lagoon and Lake Engsø

In situ diffusive water–air CO_2 and CH_4 fluxes at the shallow station GF01 near land in the western and station GF08 in the central part of Lake Engsø, as well as station GI27 in the Coastal Lagoon, were measured at monthly intervals from February to December in 2019. Water–air measurements were performed with a custom-made opaque 20 cm i.d. and 15 cm high PVC flux chamber that was kept afloat by a Styrofoam support. The flux chamber was connected by a flow-through approach to a Gasmet DX4030 Portable FTIR Ambient Gas Analyzer that monitored CO_2 and CH_4 concentrations and temperature inside the chamber continuously every 5 s for 5 min. Three sequential measurements with ambient air flushing between were performed while the flux chamber remained at each position. Water temperature was measured initially. Data was analyzed and results calculated as described above for soil-air CO_2 emission in the Coastal Lagoon before flooding.

The ebullitive water–air CH_4 emission at stations GF01 and GF08 in Lake Engsø was measured at monthly intervals from March to October (except for August) in 2019 using floating CH_4 traps (Fig. 2). The traps consisted of glass funnels with a diameter of 20 cm narrowing to 2.6 cm in a 17.5 cm long stem. The end of the stem was sealed gas tight
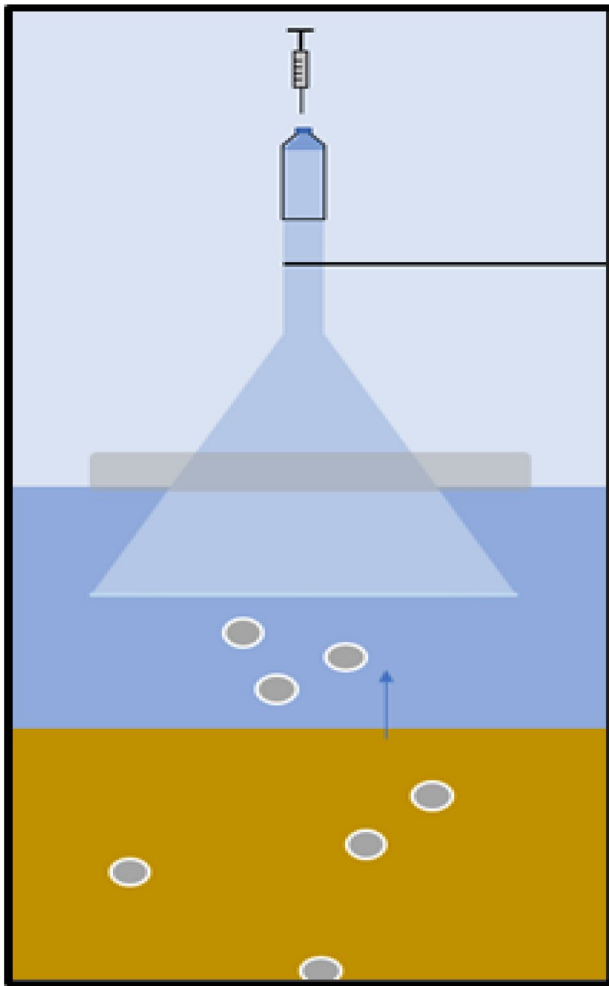
Fig. 2 Schematic drawing of floating trap for measuring ebullitive water–air CH_4 emission. It consists of an inverted glass funnel kept floating with a Styrofoam support (grey). The top is sealed gas tight with an inverted centrifuge tube (50 ml). The centrifuge tube has a scale for quantifying the amount of trapped gas. Gas samples are taken with a syringe through a rubber septum glued to the centrifuge tube

with a centrifuge tube (50 ml) which had a rubber septum glued to a hole drilled in the bottom. The traps were during deployment filled with water and turned around under water. They were kept floating with a Styrofoam support while the wide opening of the funnel stayed under water and pointing downwards. Three CH_4 ebullition traps were placed at each station and secured by a string to an anchor. After about 24 h, the volume of trapped gas was noted by a scale on the funnel stem and water temperature was measured with an electronic thermometer. Subsequently, 1 ml of the gas was sampled by a syringe with a hypodermic needle through the septum at the top of the trap and injected into a 5-ml evacuated Exetainer. The pressure in the Exetainer was in the laboratory equilibrated to 1 atm with N_2 gas and a subsample was analyzed for CH_4 by Gas Chromatography-Flame Ionization

Table 2 Monthly temperatures applied for the soil-air, soil–water, and water–air extrapolations. Air temperature is the 2015 to 2020 monthly mean measured at Odense airport by DMI. Soil temperature is air temperature corrected by the measured 1.4 °C difference between soil and air obtained during the seasonal soil-air emission survey. Lagoon water temperature is the 2015–2020 monthly mean measured at Fredericia Harbor by DMI. Lake water temperature is the 2015–2020 monthly mean in 5 shallow lakes reported by the public Danish Environmental Portal

Month	Air (°C)	Soil (°C)	Lagoon water (°C)	Lake water (°C)
Jan	2.4	3.8	3.8	3.3
Feb	2.5	3.9	2.9	3.8
Mar	4.1	5.5	3.3	4.0
Apr	7.5	8.9	6.3	6.9
May	11.8	13.2	11.4	14.0
Jun	15.7	17.1	15.7	19.4
Jul	16.7	18.1	18.1	19.6
Aug	17.4	18.8	18.1	20.1
Sep	14.1	15.5	16.1	18.1
Oct	10.1	11.5	12.3	12.4
Nov	6.1	7.5	8.9	6.9
Dec	4.8	6.2	5.4	4.9

Detection (GC-FID). The ebullitive water–air CH_4 emission (mmol m^{-2} d^{-1}) was then calculated from the CH_4 concentration in the traps after correcting for dilution in Exetainers (mM) and multiplying with trap gas volume (L) and divided by funnel area (m^2) and time (d).

Soil, Air, and Water Temperatures

To obtain estimates of the average annual soil-air CO_2 emission and soil–water DIC release for the period 2015 to 2020, the measurements performed in this study were extrapolated to mean monthly rates and summed up. Relationships between soil/water temperature and emissions/release obtained from the seasonal in situ incubations were applied to extrapolate monthly rates because temperature is assumed the primary controlling factor (Yvon-Durocher et al. 2014). For soil-air CO_2 emissions, monthly mean soil temperature is required. However, no such data are available for the area. Instead, air temperatures from 2015 to 2020 measured at Odense Airport 15 km away by DMI were converted to soil temperature by applying the measured difference in temperature between air and soil during the 2014 temporal soil-air emission survey (Table 2). For soil–water DIC release in the Coastal Lagoon, the monthly mean seawater temperatures from 2015 to 2020 measured by DMI at Fredericia Harbor 25 km away were used. Lake Engsø water temperatures were obtained as the monthly mean in

5 adjacent shallow lakes as reported by the public Danish Environmental Portal (Table 2).

Soil Characteristics

Triplicate soil cores for grain size and organic content analyses were taken with 5 cm i.d. core tubes at 30 stations in the Coastal Lagoon during 2013. Similar soil cores were taken at stations GI04 and GI27 in the Coastal Lagoon, and at stations GF01 and GF08 in Lake Engsø during 2019. Cores were in the laboratory sliced and the 0–5 cm depth interval was homogenized before subsamples were taken for analysis. Grain size of wet soil was analyzed by a Malvern Mastersizer 3000 laser diffraction system. Organic content was determined as loss-on-ignition (LOI) after combustion of dried soil samples at 520 °C for 6 h.

Porewater for SO_4^{2-} analyses was obtained from triplicate cores taken at stations GI27 and GF08 in 2019. The cores were sliced into 0–1, 1–2, 4–6, 6–8, and 10–12 cm depth intervals. Porewater was obtained by centrifugation at 3000 rpm for 10 min and filtered through GF/C filters. Subsamples were stored at 5 °C in Exetainers until analysis by HPLC anion chromatography with potassium phthalate as eluent and UV detection (precision better than 3%).

Results

Soil Conditions

The 2013 soil survey in the area that would be the coming Gyldensteen Coastal Lagoon revealed that 23 of the 30 sampling stations were located in agricultural land. These had average LOI of $3.3 \pm 0.5\%$, median grain size of 0.135 ± 0.016 mm, and silt + clay of $27.3 \pm 4.0\%$ (Table S1). Four stations (GI02, GI06, GI11, and GI29) were in manipulated areas where topsoil was removed during construction of inland dikes in preparation for the flooding. These had average LOI, median grain size, and silt + clay of $2.5 \pm 0.3\%$, 0.122 ± 0.024 mm, and $32.2 \pm 5.6\%$, respectively. Two

stations (GI08 and GI09) in a moist pasture that has never been cultivated had LOI, median grain size, and silt + clay of 23.1 and 14.7%, 0.222 and 0.191 mm, and 14.2 and 9.8%, respectively. The last station GI17 was in a deposition area near a pond formed by excavations for the original dike in 1871. This station had extremely high LOI of 64.2%, while median grain size and silt + clay were intermediate at 0.104 mm and 35.5%, respectively.

The two stations (GF01 and GF08) in Lake Engsø and the two stations in the Coastal Lagoon (GI04 and GI27) chosen for the 2019 flux measurements had remarkably similar soil characteristics with respect to median grain size that ranged from 0.151 to 0.183 mm and silt + clay within a range of 22.0 to 25.4% (Table 3). LOI, on the other hand, differed with lower values in Lake Engsø than the Coastal Lagoon. Soil conditions at GI04 and GI27 did not change significantly from 2013 to 2019, but the wave exposed GI27 showed a trend for LOI and fine particle loss.

Porewater SO_4^{2-} was constant with depth in the upper 12 cm of the soil at both GI27 and GF08. However, the concentration of SO_4^{2-} was 1–2 orders of magnitude higher in the saline GI27 soil (16.8 mM) than the freshwater dominated GF08 soil (0.4 mM) (Table 3).

Soil-Air Emission

Mapping of dark soil-air CO_2 emission in the Coastal Lagoon area before flooding conducted in September 2013 (temperature ~15 °C) revealed rates ranging from 143 to 805 mmol m^{-2} d^{-1} with an average of 405 ± 165 mmol m^{-2} d^{-1} (Fig. 3). It should be noted that four of the stations with lowest rates (GI02, GI06, GI11, and GI29) were in manipulated areas. Temperature dependence of soil-air dark CO_2 emission determined during 2014 in an adjacent pasture showed a significant exponential increase with temperature (Fig. 4, top). This area appeared representative for the entire lagoon since the extrapolated emission for September at 15.5 °C was 420 mmol m^{-2} d^{-1}, which is similar to the average rate obtained from the September 2013 mapping. By correcting air temperature by 1.4 ± 0.9 °C as observed

Table 3 Key soil characteristics from flux stations in Lake Engsø (GF) and the Coastal Lagoon (GI) (see Fig. 1 for the exact location). The results are from 2019 and given as the average ± sd of triplicate

pooled values in the upper 5 cm for solid phase parameters and the upper 12 cm for porewater SO_4^{2-}. Solid phase data from the Coastal Lagoon obtained in 2013 is shown for comparison

| Stations	LOI (%)	sd	Grain size (mm)	sd	Silt + clay (%)	sd	SO_4^{2-} (mM)	sd
GF01	0.93	0.21	0.176	0.021	23.9	4.9	-	-
GF08	0.78	0.09	0.183	0.030	24.1	5.9	0.4	0.2
GI04	2.13	0.12	0.151	0.014	22.0	3.7	-	-
GI04 (2013)	2.38	0.12	0.150	0.003	23.8	0.7	-	-
GI27	2.24	0.44	0.144	0.052	25.4	15.9	16.8	1.7
GI27 (2013)	2.79	0.11	0.109	0.016	35.5	4.7	-	-
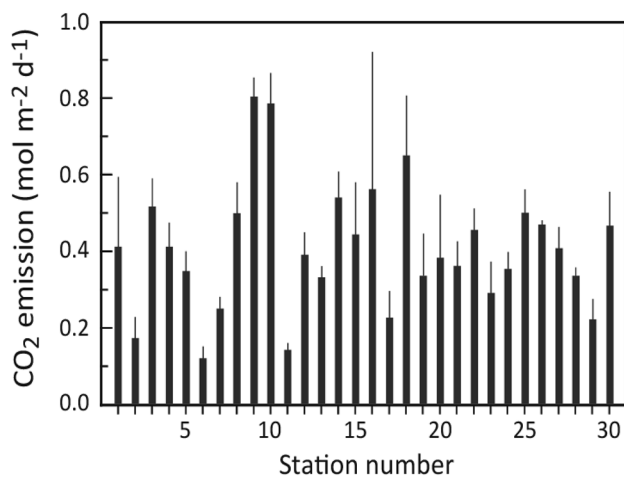
Fig. 3 The September 2013 CO_2 emissions from soil to air at 30 locations in the area that became Gyldensteen Coastal Lagoon in 2014. Rates are given average $\pm$ SD ($n=3$). Station numbers have the prefix GI in the text

during the seasonal survey in the adjacent field, the monthly average dark emission for the Coastal Lagoon area was extrapolated to range from 127 mmol m^{-2} d^{-1} in January to 590 mmol m^{-2} d^{-1} in August. After correcting to CO_2 mass, the area integrated (214 ha) total monthly dark emission in 2013 before flooding ranged from 360 Mg CO_2 in January to 1666 Mg CO_2 in August (Fig. 5), leading to an annual dark emission of ~10,300 Mg CO_2 from the Coastal Lagoon area and ~17,200 Mg CO_2 when the area of Lake Engsø is included.

Soil–Water Release

Dark soil–water DIC release that represented microbial soil respiration (RSP) at the flooded stations GI04 and GI27 in the Coastal Lagoon varied seasonally in a similar pattern between stations and among years from 2015 to 2020. Lowest RSP was recorded in winter with average dark rates of 34.3 ± 16.6 mmol m^{-2} d^{-1} at GI04 and 34.4 ± 7.8 mmol m^{-2} d^{-1} at GI27, and highest release in summer with average rates of 103.4 ± 29.5 mmol m^{-2} d^{-1} at GI04 and 108.7 ± 28.5 mmol m^{-2} d^{-1} at GI27 (Fig. 6). In addition to the strong similarity in soil–water RSP between these two stations, they also appeared representative for the entire Coastal Lagoon. Their September 2013 soil-air dark CO_2 emission of 414 ± 89 mmol m^{-2} d^{-1} (GI04) and 408 ± 113 mmol m^{-2} d^{-1} (GI27) were almost identical to the average for the entire Coastal Lagoon. The seasonal soil–water dark DIC release at these two stations showed similar strong and significant exponential increases with temperature (Fig. 4, bottom). By applying these relationships for the entire Coastal Lagoon and correcting for CO_2 mass,
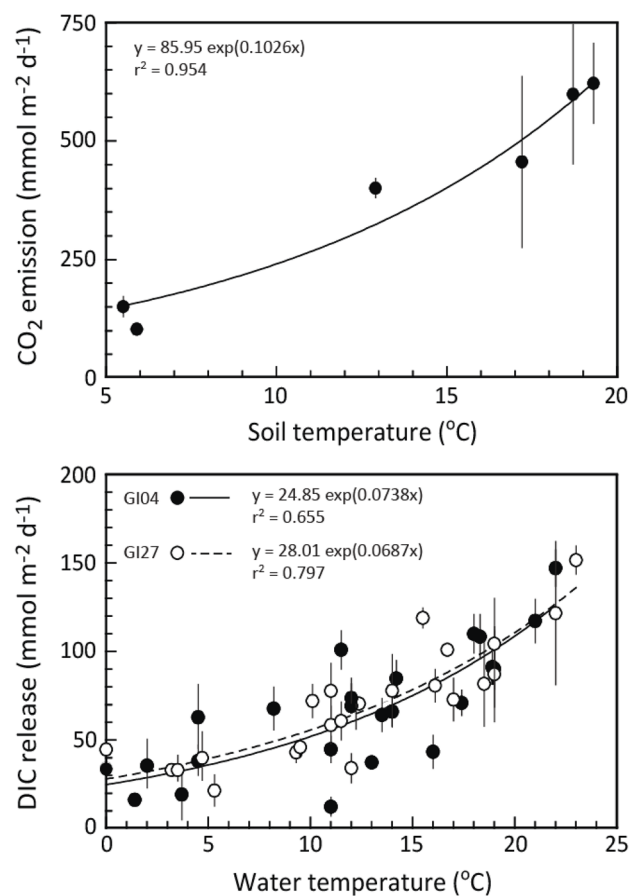

Fig. 4 Temperature dependence of soil-air CO_2 emission from unflooded agricultural land in 2014 (upper) and of seasonal soil–water DIC release at station GI04 and GI27 in the flooded Gyldensteen Coastal Lagoon from 2015 to 2020 (lower). The exponential relationships are presented by the inserted equations. Values are averages $\pm$ SD ($n=3$ (upper) and 6 (lower))

the area integrated total monthly RSP after flooding ranged from 92 Mg CO_2 in February to 271 Mg CO_2 in August (Fig. 5), leading to a potential annual emission of ~2000 Mg CO_2 from the entire 214 ha Coastal Lagoon area.
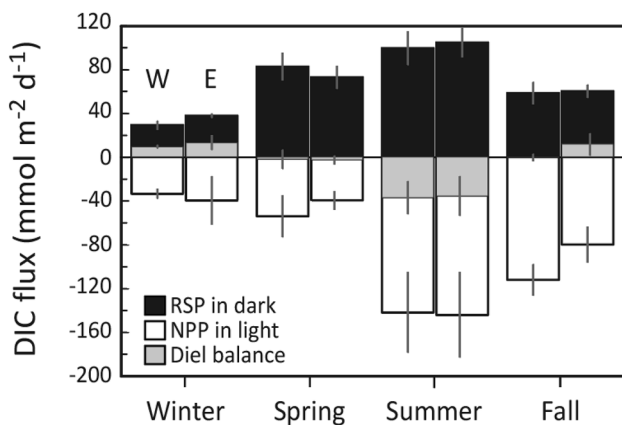
RSP in Lake Engsø obtained from measurements on soil cores from station GF08 in the laboratory ranged from 53 ± 31 mmol m^{-2} d^{-1} at 5 °C to 155 ± 17 mmol m^{-2} d^{-1} at 15 °C, which was 34 and 97%, respectively, with an average of 65% higher than obtained by the same approach at GI27 (Table 4). The contribution of Lake Engsø soil RSP to the potential annual emission from the flooded area must therefore be corrected by 65%, leading to a rate of ~2200 Mg CO_2, and thus a total ~4200 Mg CO_2 from both the Coastal Lagoon and Lake Engsø after flooding.

Soil–water DIC uptake in the light at stations GI04 and GI27 represents net primary production (NPP) by microphytobenthos in the Coastal Lagoon. NPP varied seasonally in a similar pattern between stations and among years from 2015 to 2020. Lowest NPP was recorded in
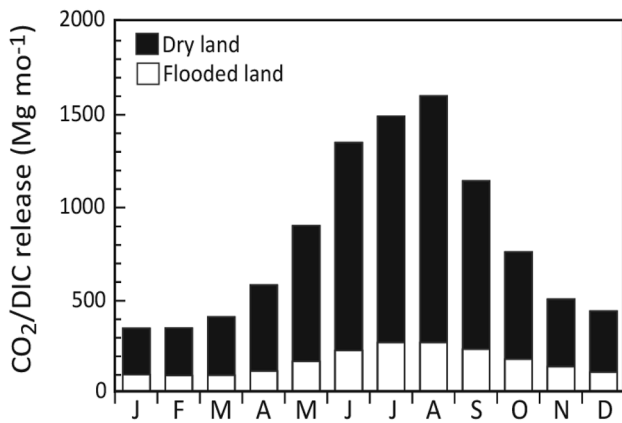
Fig. 5 Total monthly dark soil-air CO_2 emission from agricultural land before flooding in 2013 (black bars) and average dark soil–water DIC release after flooding in 2015–2020 (white bars) in Gyldensteen Coastal Lagoon. Results are estimated from measured rates and temperature dependencies using the soil and water temperatures presented in Table 2. Data are extrapolated in weight units to the entire Coastal Lagoon area (214 ha)

winter with averages of -33.4 ± 4.5 mmol m^{-2} d^{-1} at GI04 and -39.3 ± 21.8 mmol m^{-2} d^{-1} at GI27, while summer averages were as high as -140.2 ± 36.4 mmol m^{-2} d^{-1} at GI04 and -142.5 ± 38.5 mmol m^{-2} d^{-1} at GI27 (Fig. 6). Diel DIC exchange in the Coastal Lagoon was calculated as the sum of RSP and NPP, considering the dark and light hours of the relevant months and assuming that dark rates measured during daytime are fully representative for nighttime. There was a small diel net release of DIC during fall and winter with highest net rates of 9.2 ± 1.7 mmol m^{-2} d^{-1} at GI04 and 12.8 ± 6.7 mmol m^{-2} d^{-1} at GI27 in winter (Fig. 6). Conversely, a net diel DIC uptake occurred during spring and summer with highest rates in summer

of -36.0 ± 14.9 and -35.4 ± 17.9 mmol m^{-2} d^{-1} at GI04 and GI27, respectively.

CH₄ Release/Emission

Diffusive Emission
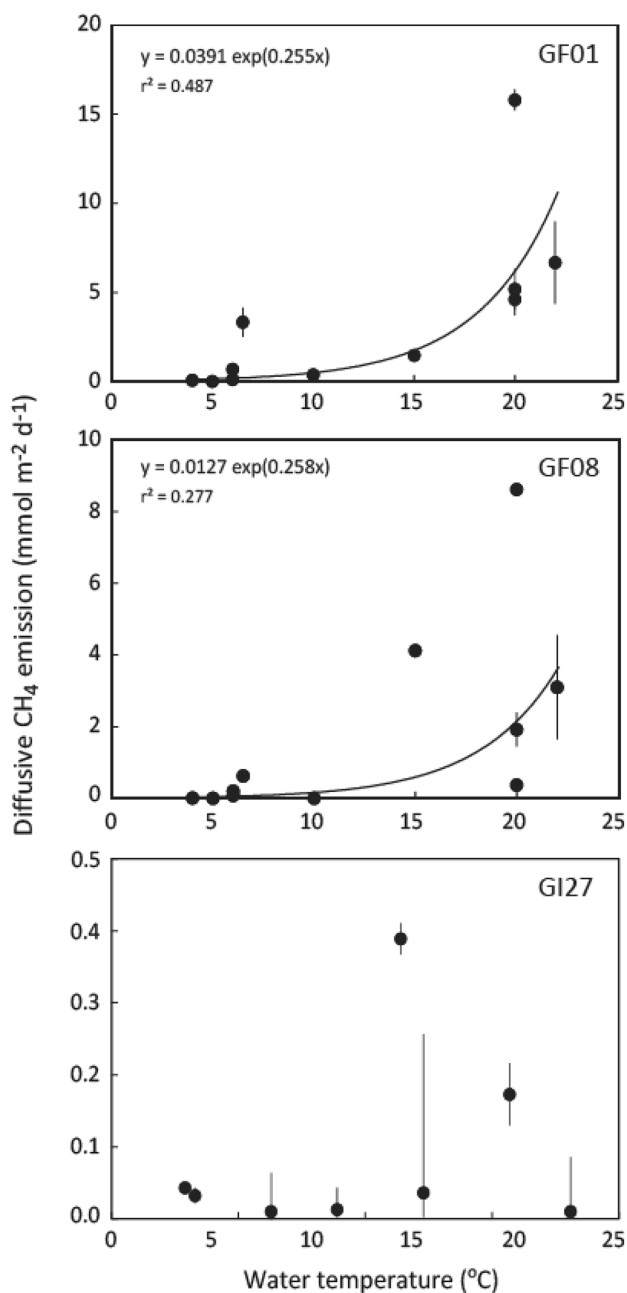
The laboratory incubations of cores from GF08 and in situ chamber measurements from GI27 showed low diffusive soil–water release of CH_4 in 2019 (< 0.4 mmol m^{-2} d^{-1}) at 5 °C and reached a high level of 57 mmol m^{-2} d^{-1} at 15 °C at GF08 but remained low at GI27 (Table 4). Diffusive in situ water–air emissions at GF01, GF08, and GI27 were also low during winter (< 0.2 mmol m^{-2} d^{-1}) and comparable to those from soil to water at low temperature. In fact, diffusive water–air emissions of CH_4 in 2019 generally remained below 1 mmol m^{-2} d^{-1} from January to April and October to December at all locations, and only reached elevated rates of up to 16 and 9 mmol m^{-2} d^{-1} at GF01 and GF08, respectively, during the warmest summer months. Consequently, significant exponential temperature relationships were evident for diffusive water–air emission of CH_4 at GF01 and GF08 (Fig. 7). According to these relationships, emissions of CH_4 were generally 3 times higher at GF01 than GF08. No exponential relationship with temperature was evident for diffusive CH_4 emission at GI27 where rates remained below 0.4 mmol m^{-2} d^{-1} throughout 2019.

The two stations examined in Lake Engsø are assumed representative for the entire lake when their areal distribution is considered. Air photos revealed that the littoral zone represented by GF01 covered about 25% of the total lake area in 2019 and the remainder 75% is represented by GF08. By applying mean temperatures in 5 adjacent shallow lakes, the monthly average diffusive CH_4 emission from GF01 and GF08 was extrapolated to range from 0.09 and 0.03 mmol m^{-2} d^{-1} in January to 6.61 and 2.28 mmol m^{-2} d^{-1} in August, respectively. After correcting to CH_4 mass and the areal distribution of GF01 and GF08, the Lake

Fig. 6 Seasonal soil–water DIC release by soil respiration in the dark (RSP, black bars) and uptake by soil net primary production (NPP, white bars) in the light at GI04 (W) and GI27 (E) from 2015 to 2020. Net diel rates are shown by grey bars. Values are given as averages ± SD ($n=6$)

Table 4 Dark soil–water release of CO_2 and CH_4 at 5 and 15 °C from station GF08 in Lake Engsø and GI27 in the Coastal Lagoon (see Fig. 1 for the exact location). The results for GF08 are derived from laboratory core incubations and compared with in situ chamber measurements from GI27. The results are from 2019 and given as the average ± sd of triplicate cores
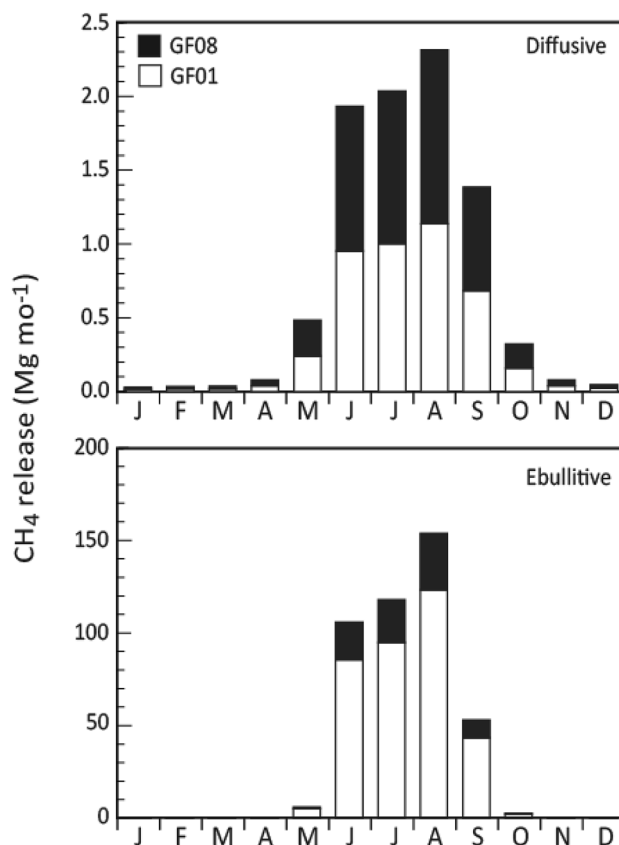
| Stations | CO_2 flux | sd | CH_4 flux | sd | Temperature |
	mmol m^{-2} d^{-1}		mmol m^{-2} d^{-1}		°C
GF08	52.5	30.6	0.34	0.42	5
GF08	155.5	41.4	57.00	2.01	15
GI27	39.2	27.0	0.35	0.42	5
GI27	78.9	36.9	0.40	0.22	15

Fig. 7 Temperature dependence of diffusive in situ water–air emissions at GF01 and GF08 in Lake Engsø and GI27 in the Coastal Lagoon. The exponential relationships are presented by the inserted equations. No significant exponential relationship could be obtained for the low rates at GI27. Values are averages $\pm$ SD ($n = 3$)


Fig. 8 Total monthly diffusive (upper) and ebullitive (lower) water–air CH_4 emission in Lake Engsøen. Results are estimated from measured rates and temperature dependencies using the water temperatures presented in Table 2. Data are extrapolated in weight units to the entire Lake Engsø area (144 ha) assuming that GF01 (white bars) is representative for 25% and GF08 (black bars) is representative for 75% of the total lake area

Engsø area integrated (144 ha) total monthly diffusive CH_4 emission ranged from 0.03 Mg in January to 2.31 Mg in August (Fig. 8, top) with almost an equal share of the littoral and basin areas. The estimated total annual diffusive emission from Lake Engsø was then ~8.8 Mg CH_4, while the contribution from the Coastal Lagoon was negligible.

Ebullitive Emission

Ebullition of CH_4 was only detected in Lake Engsø and here with a clear and strong temperature dependence. Very little water–air CH_4 emission through ebullition was evident at temperatures below 10 °C (< 1 mmol m^{-2} d^{-1}). Ebullition increased considerably above this temperature reaching 482–590 mmol m^{-2} d^{-1} at GF01 and 67–205 mmol m^{-2} d^{-1} at GF08 in July–September. The associated significant exponential relationship was very steep (Fig. 9) with about 10 times higher ebullition at GF01 than GF08 at 20 °C. After the appropriate corrections to CH_4 mass and the areal distribution of GF01 and GF08, total monthly ebullitive CH_4 emission ranged from 0.01 Mg in January to 105 Mg in August (Fig. 8, bottom) with about 4 times higher share from the littoral than the basin areas. The estimated total annual ebullitive emission from Lake Engsø was then ~294 Mg CH_4.
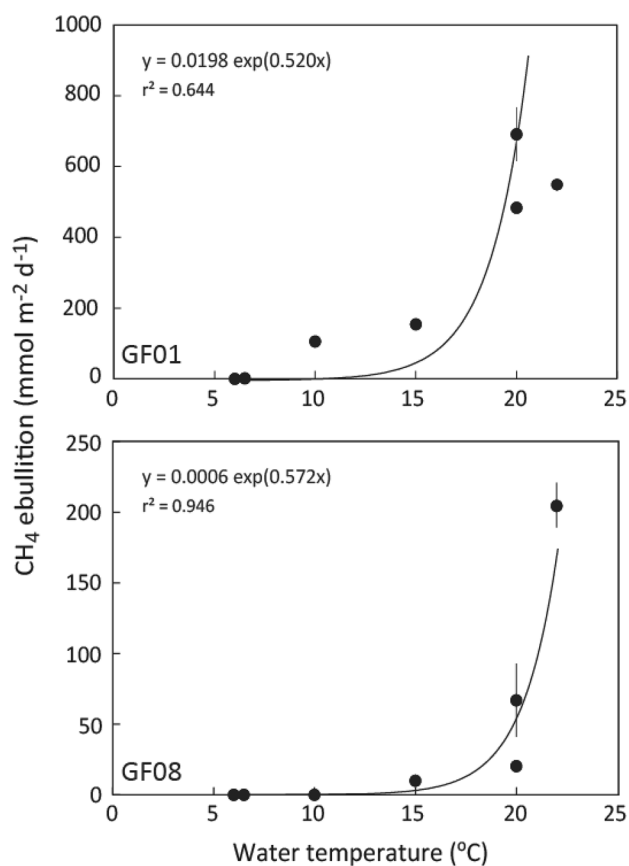
Fig. 9 Temperature dependence of ebullitive in situ water–air emissions at GF01 and GF08 in Lake Engsø. The exponential relationships are presented by the inserted equations. Values are averages $\pm$ SD ($n=3$)

Discussion

CO_2 Dynamics

Cultivated agricultural land emits large amounts of CO_2 to the atmosphere driven by aerobic micro- and macro-heterotrophic carbon mineralization within the oxic soil (Trumbore 2006; Maljanen et al. 2007; FAO 2022). The average CO_2 emissions of 405 ± 165 mmol m^{-2} d^{-1} observed here for the Gyldensteen farmland before 2014 (Fig. 3) are within the range reported by other studies that have assessed respiration rates from agricultural soils (Lohila et al. 2003; Lai et al. 2012). Elsgaard et al. (2012) reported annual ecosystem respiration ranging from 5.3 to 12.2 kg CO_2 m^{-2} in 8 organic agricultural soils from Denmark. This corresponds to a range of 330–759 mmol CO_2 m^{-2} d^{-1} and is comparable to emissions reported in this study. The spatial variation in emissions among locations as observed in the present study and by others is caused by differences in soil characteristics, such as grain size, water, organic, and nutrient content as well as preceding agricultural practice.

Soil water content affects soil respiration rates and is closely linked to precipitation. Gas diffusivity, and thus oxygen availability in the soil, varies inversely with water content (Huesemann and Truex 1996). Microbial respiration is therefore inhibited when soils are water saturated (Liu et al. 2009). Under drained conditions, there is a wide range of water contents within which only small changes exist in respiration rate, but as the soil dries completely, there is a threshold below which microbial activity is inhibited, and respiration decreases (Smith et al. 2018). However, the soils in the Gyldensteen area were not water saturated but remained sufficiently moist during the study period before flooding to maintain a steady respiration and CO_2 emission (Table S1).

Organic content in Gyldensteen soils varied before flooding with most locations having LOI ranging from 1.4 to 6.6% and must be categorized at the transition between mineral soils and mineral soils with organics (Table S1) (El Howayek et al. 2012). The Gyldensteen agricultural area has been under conventional management for 150 years and has during this period likely lost much of its carbon pool, due to agriculture practices such as deep-going and frequent tillage (Reicosky et al. 1997; Grant et al. 2004; Smith et al. 2010). Conventional management has been shown to lead to higher microbial derived CO_2 fluxes and to exhaustion of the organic pools compared with conservation systems (Smith et al. 2010).

Conversely, farmland crops will certainly also assimilate CO_2 and convert it into plant biomass. NPP of crops must be included in estimates of farmland GHG balance. Since no data are available of NPP from the Gyldensteen farmland prior to 2014, net CO_2 emission estimates can only be derived from published NPP of crops similar to those cultivated at Gyldensteen and compared to published net ecosystem emissions published from cultivated sites comparable to the Gyldensteen area. Ciais et al. (2010) reported NPP in European croplands of 451–595 g C m^{-2} yr^{-1} C. This corresponds to a total NPP in the 358 ha Gyldensteen cultivated area of 5900–7800 Mg CO_2 yr^{-1}. This NPP estimate is equivalent to 34–45% of the total dark CO_2 emissions of 17,200 Mg CO_2 yr^{-1} estimated here, leaving an annual net CO_2 loss from the total Gyldensteen area of roughly 9300 to 11,200 Mg CO_2 yr^{-1}. According to this estimate, the Gyldensteen agricultural area was a large net CO_2 emitter before flooding, within the range reported by Elsgaard et al. (2012) and others (Kasimir-Klemedtsson et al. 1997; Freibauer et al. 2004; Janssens et al. 2005).

When agricultural soil is flooded, the condition for microbial decay is severely altered. While aerated and well-drained soils have rapid oxygen diffusion depths of up to 1 m (Megonigal et al. 1993), the water filled pore spaces in flooded soils slow oxygen diffusion by a factor of 10^4 (Megonigal et al. 2004). Accordingly, aerobic decomposition and associated CO_2

production is severely hampered (Hackney 1987; Kristensen et al. 1995; Kirwan and Blum 2011). This response to flooding was evident at Gyldensteen Coastal Lagoon where dark DIC release was 75% slower than the CO_2 emission before flooding (Fig. 5). This change in RSP upon flooding is consistent with other studies carried out in restored wetlands (Blackwell et al. 2002; Sjøgaard et al. 2017; Pendleton et al. 2012; Wollenberg et al. 2018).

The overall CO_2 balance of the Gyldensteen area after flooding must include the contribution of aquatic primary producers in the light before concluding whether the area is a sink or a source of CO_2. The measurements of DIC/CO_2 exchange performed at the soil–water and the water–air interface in both the Coastal Lagoon and Lake Engsø clearly indicate that the uptake of CO_2 by aquatic primary producers (primarily microphytobenthos) on an annual basis completely matches the release of CO_2 by soil RSP (Fig. 6). Thus, the net CO_2 emission has changed from 10,350 Mg yr^{-1} before flooding to virtually zero after flooding and in the year 2019, the Coastal Lagoon was actually a small sink of CO_2. Conservatively, we consider that the net emission from the area is 0 to allow for interannual variation in fluxes. A similar balance or even net uptake of CO_2 after flooding has been documented in various types of restored wetlands (Knox et al. 2015; Hemes et al. 2018; Welsh et al. 2021). Valach et al. (2021) found that restored wetlands can be strong C sinks 2 years after restoration with a vegetation cover > 55%. Thus, the Gyldensteen area may in the future improve its carbon sequestering ability trough increased vegetation establishment.

The soil–water DIC fluxes appeared higher in Lake Engsø than the Coastal Lagoon (Table 4). This is probably due to high availability of labile substrates generated by higher phytoplankton production in the nutrient-rich Lake Engsø environment. The soils of the Coastal Lagoon and Lake Engsø were similar before flooding, but conditions in the two wetlands developed differently following flooding. The Coastal Lagoon is an open system with short water residence time that prevents nutrient accumulation and high phytoplankton production (Kristensen et al. 2021). The higher CO_2 formation in Lake Engsø may be counteracted by a generally higher photosynthetic CO_2. Thus, Huttunen et al. (2003) demonstrated that CO_2 emissions from eutrophic lakes are larger than from oligotrophic lakes. The overall balance in Lake Engsø is not fully elucidated from the present measurements because soil–water DIC fluxes of practical reasons were measured in darkened cores under laboratory conditions.

CH₄ Dynamics

Soil CH_4 flux is controlled by a balance between methanogenesis and methanotrophy in combination with CH_4 diffusivity (von Fischer et al. 2009). Although no measurements were made of soil-air CH_4 fluxes in the Gyldensteen area prior to flooding, it is assumed negligible. Methanogenesis is a strictly anaerobic microbial process that typically takes place several meters down in well-drained soils. All the produced CH_4 will therefore be oxidized during diffusive transit in the oxic upper layers of the soil before reaching the atmosphere (Topp and Pattey 1997). In fact, Skinner et al. (2014) reported net uptake of CH_4 in several oxic agricultural soils.

After flooding, the zone of methanogenesis may move up to a few mm below the soil-surface. This typically occurs when soils are flooded with freshwater devoid of SO_4^{2-}, leading to considerable release of CH_4 to the overlying water and subsequently emission to the atmosphere (Sha et al. 2011; Sanchez-Rodriguez et al. 2019; Schindler et al. 2020). CH_4 is simply transported too fast over a short distance that it, to a large extent, bypasses the narrow upper oxic zone of the soil with active methanotrophy (Jeffrey et al. 2019). If soils are flooded with seawater containing high concentrations of SO_4^{2-}, microbial sulfate reduction competitively inhibits methanogenesis in the upper tenths of cm in the soil (Abram and Nedwell 1978; Ding and Cai 2004; Livesley and Andrusiak 2012). Most of the CH_4 generated deeper in the soil is therefore oxidized by methanotrophic sulfate reducers while diffusing upwards in the soil, leaving almost no release to the overlying water. This explains the large difference in diffusive soil–water release of CH_4 during summer between Lake Engsø (57 mmol m^{-2} d^{-1}) and the Coastal Lagoon (0.4 mmol m^{-2} d^{-1}) (Table 4, Fig. 7). Other studies support these findings and report that restored freshwater wetlands are large CH_4 emitters (Herbst et al. 2011; Bridgham et al. 2013; Knox et al. 2015; Hemes et al. 2018).

Measurement of ebullitive CH_4 emission is challenging due to the large spatial and temporal variation of bubble releases (Soumis et al. 2004; Baron et al. 2022). However, it is essential to include ebullitive CH_4 emissions in GHG budgets of freshwater wetlands because it may contribute greatly to the total, and in some cases, dominate CH_4 emission (Wik et al. 2013; Delsontro et al. 2016; Wu et al. 2019; Taoka et al. 2020; Wang et al. 2021). This was certainly the case in Lake Engsø during summer where ebullitive water–air CH_4 emission was about 100 times higher than diffusive CH_4 emission (Fig. 8). CH_4 ebullition typically occurs when CH_4 concentrations in soil porewaters exceed the solubility threshold, particularly during periods of low atmospheric pressure (Zhao et al. 2022). Since transport of CH_4 bubbles from the soil–water interface to the water–air interface is much faster than the diffusive transport, much less CH_4 is oxidized in the water column. In contrast, less than 10% of the diffusive soil–water CH_4 release (Table 4) is emitted across the water–air interface (Fig. 7) due to oxidation during transit within the water column.

Table 5 CO_2 emission and CH_4 emission before and after flooding in the Coastal Lagoon and Lake Engsø. CO_2 dark emission (DE) and net emission (NE) is presented+diffusive and ebullitive CH_4 emission. In the two rows at the bottom, the GHG balance is given as CO_2-equivalents

	Before flooding 2013		After flooding 2019	
	Coastal Lagoon	*Freshwater Lake*	*Coastal Lagoon*	*Freshwater Lake*
CO_2 (Mg yr^{-1}) (DE)	10,300	6,900	2,000	2,200
CO_2 (Mg yr^{-1}) (NE)	6,210	4,140	−70	−78
CH_4 diffusive (Mg yr^{-1})	~0	~0	~0	8.8
CH_4 ebullition (Mg yr^{-1})	~0	~0	~0	294
CO_2 equivalents (Mg yr^{-1})	6,210	4,140	−70	8,400
CO_2 equivalents (Mg yr^{-1})	**10,350**		**8,330**	

Evidence from this study and others confirms that temperature is a major controlling factor for CH_4 emissions (Gedney et al. 2004; Pelletier et al. 2007; Turetsky et al. 2008; Tagesson et al. 2012; Yvon-Durocher et al. 2014). Geng et al. (2019) found that an exponential relation with increasing temperature was the best fit for projections of CH_4 emissions. The apparent exponential fit of both diffusive and ebullitive CH_4 emission with temperature in Lake Engsø (Figs. 7, 9) supports this contention. It is striking, though, that both CH_4 emission pathways were hardly detectable below 10 °C and increases steeply above this temperature threshold, particularly for ebullitive emission. Similarly, Jansen et al. (2020) found the same temperature dependence for both pathways in Norwegian lakes and noticed that they were virtually independent of temperature below 6 °C. However, the use of the steep exponential fits to extrapolate total annual ebullitive emissions from temperature records must be expected to have large uncertainty (Fig. 9). It is particularly critical at high temperature where the estimated CH_4 ebullition from stations GF01 and GF08 increases by 68 and 77%, respectively, when temperature increases from 20 to 21 °C. Thus, our total annual diffusive and ebullitive CH_4 emission estimates of 8.8 and 294 Mg CH_4 yr^{-1} must be considered with care, but still remain within the right order of magnitude. Nevertheless, the steep exponential increase in CH_4 emission by both pathways at temperatures around 20 °C has serious implications when considering the proposed temperature rise of 1.1–5.4 °C due to global warming within the next 100 years (Solomon et al. 2007).

It should be noted, though, that CH_4 emission is not solely controlled by temperature. Both diffusive and ebullitive emission of CH_4 also depend on factors like soil organic content and water table height (Christensen et al. 2003; Calabrese et al. 2021). Thus, the high CH_4 emissions from Lake Engsø are in part caused by the fact that it is shallow, but also that the system is eutrophic with high levels of labile organic matter deposits in the soil. Accordingly, Yagi and Minami (1991) found that exogenous supplies of organic carbon have direct bearing on CH_4 production in waterlogged soils. However, the limited variation of organic content within Lake Engsø precludes any evaluation of its role for CH_4 emission in the present study.

GHG Balance

The GHG balance in the entire Gyldensteen area before and after flooding can be assessed by comparing the uptake and emission of CO_2 and CH_4 in CO_2-equivalents using a CH_4 GWP of 28 (IPCC 2007). Before flooding in 2013, the total area was a net source of about 10,350 Mg CO_2-e. yr^{-1} (Table 5). In 2019, the area remained a source of GHG with a net emission of 8330 Mg CO_2-e yr^{-1}. The post-flooding net emission was almost solely caused by high ebullitive and diffusive CH_4 emissions in Lake Engsø during summer as net CO_2 emissions were practically zero (Table 5). While GHG mitigation by flooding in the Coastal Lagoon accounted for 6280 Mg CO_2-e yr^{-1}, Lake Engsø increased the GHG emissions by about 100% (from 4140 to 8400 Mg CO_2-e yr^{-1}). Thus, total GHG-emissions in the entire area (Coastal Lagoon and Lake Engsø) were reduced by no more than about 20% after flooding. Had the entire area been flooded with seawater, the total annual post-flooding net emission of CO_2-e may have been close to zero. Accordingly, the GHG mitigation in the restored wetlands at Gyldensteen is greatly diminished by the CH_4 emission from Lake Engsø.

Conclusions

The present study clearly emphasizes that flooding of agricultural land with either seawater or freshwater has large impacts on GHG emissions. Soil anoxia induced by flooding decreased net CO_2 emissions to virtually zero, providing a GHG mitigation of ~29 Mg CO_2 ha^{-1} yr^{-1}, which strongly confirms our hypothesis 1. However, this mitigation capacity was only reached to its full extent in Gyldensteen Coastal Lagoon that was flooded with seawater. In these soils, sulfate reduction prevented CH_4 formation within and emission from the soil. In Lake Engsø, that was flooded with freshwater, methanogenesis and rapid transport of CH_4 (diffusive and ebullitive) doubled GHG emissions from 29 to

58 Mg CO_2-e ha^{-1} yr^{-1}, which confirms our hypothesis 2. The large variation of CO_2 and CH_4 release on temporal scales depended strongly on temperature, which confirms our hypothesis 3. It is particularly worth noting that there were very strong dependencies of CH_4 ebullition on temperature with significant exponential trends.

References

Abernethy, S., and R.B. Jackson. 2022. Global temperature goals should determine the time horizons for greenhouse gas emission metrics. *Environmental Research Letters* 17: 024019. https://doi.org/10.1088/1748-9326/ac4940.

Abram, J.W., and D.B. Nedwell. 1978. Inhibition of methanogenesis by sulphate reducing bacteria competing for transferred hydrogen. *Archives of Microbiology* 117: 89–92.

Arias-Ortiz, A., P.Y. Oikawa, J. Carlin, P. Masqué, J. Shahan, S. Kanneg, A. Paytan, and D.D. Baldocchi. 2021. Tidal and nontidal marsh restoration: a trade-off between carbon sequestration, methane emissions, and soil accretion. *Journal of Geophysical Research: Biogeosciences* 126: e2021JG006573. https://doi.org/10.1029/2021JG006573.

Andrews, J.E., D. Burgess, R.R. Cave, E.G. Coombes, T.D. Jickells, D.J. Parkes, and R.K. Turner. 2006. Biogeochemical value of managed realignment, Humber estuary, UK. *Science of the Total Environment* 371: 19–30.

Baron, A.A.P., L.T. Dyck, H. Amjad, J. Bragg, E. Kroft, J. Newson, K. Oleson, N.J. Casson, R.L. North, J.J. Venkiteswaran, and C.J. Whitfield. 2022. Differences in ebullitive methane release from small, shallow ponds present challenges for scaling. *Science of The Total Environment* 802: 149685. https://doi.org/10.1016/j.scitotenv.2021.149685.

Bastviken, D., L.J. Tranvik, J.A. Downing, P.M. Crill, and A. Enrich-Prast. 2011. Freshwater methane emissions offset the continental carbon sink. *Science* 331: 50–50. https://doi.org/10.1126/science.1196808.

Benbi, D.K. 2013. Greenhouse gas emissions from agricultural soils: Sources and mitigation potential. *Journal of Crop Improvement* 27: 752–772.

Blackwell, M.S.A., D.V. Hogan, and E. Maltby. 2002. Wetlands as regulators of pollutant transport. *CAB International. Agriculture, Hydrology and Water Quality* (eds P.M. Haygarth and S.C. Jarvis). https://doi.org/10.1079/9780851995458.0321.

Bridgham, S.D., H. Cadillo-Quiroz, J.K. Keller, and Q. Zhuang. 2013. Methane emissions from wetlands: Biogeochemical, microbial, and modeling perspectives from local to global scales. *Global Change Biology* 19: 1325–1346.

Burden, A., R.A. Garbutt, C.D. Evans, D.L. Jones, and D.M. Cooper. 2013. Carbon sequestration and biogeochemical cycling in a saltmarsh subject to coastal managed realignment. *Estuarine, Coastal and Shelf Science* 120: 12–20.

Cadier, C., E. Bayraktarov, R. Piccolo, and M.F. Adame. 2020. Indicators of coastal wetlands restoration success: a systematic review. *Frontiers in Marine Science* 7. https://doi.org/10.3389/fmars.2020.600220.

Calabrese, S., A. Garcia, J.L. Wilmoth, X. Zhang, and A. Porporato. 2021. Critical inundation level for methane emissions from wetlands. *Environmental Research Letters* 16(4): [044038]. https://doi.org/10.1088/1748-9326/abedea

Canfield, D.E., E. Kristensen, and B. Thamdrup. 2005. *Aquatic geomicrobiology*. Academic Press.

Chimner, R.A., D.J. Cooper, F.C. Wurster, and L. Rochefort. 2017. An overview of peatland restoration in North America: Where are we after 25 years? *Restoration Ecoogy* 25: 283–292. https://doi.org/10.1111/rec.12434.

Chmura, G.L., S.C. Anisfeld, D.R. Cahoon, and J.C. Lynch. 2003. Global carbon sequestration in tidal, saline wetland soils. *Global Biogeochemical Cycles* 17: 1111. https://doi.org/10.1029/2002GB001917.

Christensen, T. R., A. Ekberg, L. Ström, M. Mastepanov, N. Panikov, M. Öquist, B.H. Svensson, H. Nykänen, P.J. Martikainen, and H. Oskarsson. 2003. Factors controlling large scale variations in methane emissions from wetlands. *Geophysical Research Letters* 30: 7 1414. https://doi.org/10.1029/2002GL016848.

Ciais, P., M. Wattenbach, N. Vuichard, P. Smith, S.L. Piao, A. Don, S. Luyssaert, I. A. Janssens, A. Bondeau, R. Dechow, A. Leip, P.C. Smith, C. Beer, G.R. van der Werf, S. Gervois, K. van Oost, E. Tomelleri, A. Freibauer, E.D. Schulze, Carboeurope Synthesis Team. 2010. The European carbon balance. Part 2: Croplands. *Global Change Biology* 16: 1409–1428. https://doi.org/10.1111/j.1365-2486.2009.02055.x.

Crooks, S., D. Herr, J. Tamelander, D. Laffoley, and J. Vandever. 2011. Mitigating climate change through restoration and management of coastal wetlands and near-shore marine ecosystems: challenges and opportunities. *Environment Department Paper* 121. World Bank, Washington, DC.

Davidson, N.C. 2014. How much wetland has the world lost? Long-term and recent trends in global wetland area. *Marine and Freshwater Research* 65: 934–941.

Davidson, T.A., J. Audet, E. Jeppesen, F. Landkildehus, T.L. Lauridsen, M. Søndergaard, and J. Syväranta. 2018. Synergy between nutrients and warming enhances methane ebullition from experimental lakes. *Nature Climate Change* 8: 156–160. https://doi.org/10.1038/s41558-017-0063-z.

DelSontro, T., L. Boutet, A. St-Pierre, P. Giorgio, and Y. Prairie. 2016. Methane ebullition and diffusion from northern ponds and lakes regulated by the interaction between temperature and system productivity. *Limnology and Oceanography* 61: S62–S77. https://doi.org/10.1002/lno.10335.

Ding, W.X., and Z.C. Cai. 2007. Methane emission from natural wetlands in China: Summary of years 1995–2004 studies. *Pedosphere* 17: 475–486. https://doi.org/10.1016/s1002-0160(07)60057-5.

El Howayek, A., A. Bobet, S. Dawood, A. Ferdon, M. Santagata, and N.Z. Siddiki. 2012. Project implementation: classification of organic soils and classification of marls—training of INDOT personnel. Publication FHWA/IN/JTRP-2012/22. Joint Transportation Research Program, Indiana Department of Transportation and Purdue University, West Lafayette, Indiana. https://doi.org/10.5703/1288284314984.

Elsgaard, L., C.M. Gorres, C.C. Hoffmann, G. Blicher-Mathiesen, K. Schelde, and S.O. Petersen. 2012. Net ecosystem exchange of CO_2 and carbon balance for eight temperate organic soils under agricultural management. *Agriculture Ecosystems & Environment* 162: 52–67.

FAO. 2022. Greenhouse gas emissions from agrifood systems. Global, regional and country trends, 2000–2020. FAOSTAT Analytical Brief Series No. 50. Rome, FAO.

Freibauer, A., M.D.A. Rounsevell, P. Smith, and J. Verhagen. 2004. Carbon sequestration in the agricultural soils of Europe. *Geoderma* 122: 1–23.

Gedan, K.B., M.L. Kirwan, E. Wolanski, E.B. Barbier, and B.R. Silliman. 2011. The present and future role of coastal wetland vegetation in protecting shorelines: Answering recent challenges to the paradigm. *Climatic Change* 106: 7–29.

Gedney, N., P.M. Cox, and C. Huntingford. 2004. Climate feedback from wetland methane emissions. *Geophysical Research Letters* 31: L20503.

Geng, M.S., J.H. Christensen, and T.R. Christensen. 2019. Potential future methane emission hot spots in Greenland. *Environmental Research Letters* 14: 035001. https://doi.org/10.1088/1748-9326/aaf34b.

Grant, B., W.N. Smith, R. Desjardins, R. Lemke, and C. Li. 2004. Estimated N_2O and CO_2 emissions as influenced by agricultural practices in Canada. *Climatic Change* 65: 315–332. https://doi.org/10.1023/b:Clim.0000038226.60317.35.

Hackney, C.T. 1987. Factors affecting accumulation or loss of macroorganic matter in salt marsh sediments. *Ecology* 68: 1109–1113.

Hall, P.J., and R.C. Aller. 1992. Rapid, small-volume, flow injection analysis for ΣCO_2, and NH_4^+ in marine and freshwaters. *Limnology and Oceanography* 37: 1113–1119.

Hartvigsen, M.B. 2014. Land consolidation and land banking in Denmark: Tradition, multi-purpose and perspectives. *Danish Journal of Geoinformatics and Land Management* 47: 51–73.

Hemes, K.S., S.D. Chamberlain, E. Eichelmann, S.H. Knox, and D.D. Baldocchi. 2018. A biogeochemical compromise: The high methane cost of sequestering carbon in restored wetlands. *Geophysical Research Letters* 45: 6081–6091. https://doi.org/10.1029/2018gl077747.

Herbst, M., T. Friborg, R. Ringgaard, and H. Soegaard. 2011. Interpreting the variations in atmospheric methane fluxes observed above a restored wetland. *Agricultural and Forest Meteorology* 151: 841–853. https://doi.org/10.1016/j.agrformet.2011.02.002.

Huesemann, M.H., and M.J. Truex. 1996. The role of oxygen diffusion in passive bioremediation of petroleum contaminated soils. *Journal of Hazardous Materials* 51: 93–113. https://doi.org/10.1016/s0304-3894(96)01834-1.

Huttunen, J.T., J. Alm, A. Liikanen, S. Juutinen, T. Larmola, T. Hammar, J. Silvola, and P.J. Martikainen. 2003. Fluxes of methane, carbon dioxide and nitrous oxide in boreal lakes and potential anthropogenic effects on the aquatic greenhouse gas emissions. *Chemosphere* 52: 609–621. https://doi.org/10.1016/S0045-6535(03)00243-1.

IPCC. 2007. Climate change 2007: synthesis report. Contribution of Working Groups I, II and III to the Fourth Assessment Report of the Intergovernmental Panel on Climate Change [Core Writing Team, Pachauri, R.K and Reisinger, A. (eds.)]. IPCC, Geneva, Switzerland, 104 pp.

Jansen, J., B.F. Thornton, M. Wik, S. MacIntyre, and P.M. Crill. 2020. Temperature proxies as a solution to biased sampling of lake methane emissions. *Geophysical Research Letters* 47: e2020GL088647. https://doi.org/10.1029/2020GL088647.

Janssens, I.A., A. Freibauer, B. Schlamadinger, R. Ceulemans, P. Ciais, A.J. Dolman, M. Heimann, G.J. Nabuurs, P. Smith, R. Valentini, and E.D. Schulze. 2005. The carbon budget of terrestrial ecosystems at country-scale - a European case study. *Biogeosciences* 2: 15–26.

Jeffrey, L.C., D.T. Maher, S.G. Johnston, K. Maguire, A.D.L. Steven, and D.R. Tait. 2019. Rhizosphere to the atmosphere: Contrasting methane pathways, fluxes, and geochemical drivers across the terrestrial-aquatic wetland boundary. *Biogeosciences* 16: 1799–1815. https://doi.org/10.5194/bg-16-1799-2019.

Jørgensen, B.B. 2006. Bacteria and marine biogeochemistry. In *Marine Geochemistry*, ed. H.D. Schulz and M. Zabel, 173–207. Berlin/Heidelberg: Springer-Verlag.

Kasimir-Klemedtsson, A., L. Klemedtsson, K. Berglund, P. Martikainen, J. Silvola, and O. Oenema. 1997. Greenhouse gas emissions from farmed organic soils: A review. *Soil Use and Management* 13: 245–250. https://doi.org/10.1111/j.1475-2743.1997.tb00595.x.

Kirwan, M.L., and L.K. Blum. 2011. Enhanced decomposition offsets enhanced productivity and soil carbon accumulation in coastal wetlands responding to climate change. *Biogeosciences* 8: 987–993.

Knox, S.H., C. Sturtevant, J.H. Matthes, L. Koteen, J. Verfaillie, and D. Baldocchi. 2015. Agricultural peatland restoration: Effects of land-use change on greenhouse gas (CO_2 and CH_4) fluxes in the Sacramento-San Joaquin Delta. *Global Change Biology* 21: 750–765. https://doi.org/10.1111/gcb.12745.

Kristensen, E., S.I. Ahmed, and A.H. Devol. 1995. Aerobic and anaerobic decomposition of organic matter in marine sediment: Which is fastest? *Limnology and Oceanography* 40: 1430–1437.

Kristensen, E., C.O. Quintana, T. Valdemarsen, and M.R. Flindt. 2021. Nitrogen and phosphorus export after flooding of agricultural land by coastal managed realignment. *Estuaries and Coasts* 44: 657–671. https://doi.org/10.1007/s12237-020-00785-2.

Kroeger, K.D., S. Crooks, S. Moseman-Valtierra, and J. Tang. 2017. Restoring tides to reduce methane emissions in impounded wetlands: A new and potent Blue Carbon climate change intervention. *Scientific Reports* 7: 1–12. https://doi.org/10.1038/s41598-017-12138-4.

Laanbroek, H.J. 2010. Methane emission from natural wetlands: Interplay between emergent macrophytes and soil microbial processes. *A Mini-Review. Annals of Botany* 105: 141–153.

Lai, L., X. Zhao, L. Jiang, Y. Wang, L. Luo, Y. Zheng, X. Chen, and G.M. Rimmington. 2012. Soil respiration in different agricultural and natural ecosystems in an arid region. PLoS ONE 7: e48011. https://doi.org/10.1371/journal.pone.0048011.

Lal, R. 2008. Sequestration of atmospheric CO_2 in global carbon pools. *Energy & Environmental Science* 1: 86–100.

Li, X., R. Bellerby, C. Craft, and S.E. Widney. 2018. Coastal wetland loss, consequences, and challenges for restoration. *Anthropocene Coasts* 1: 1–15.

Liu, W., Z. Zhang, and S. Wan. 2009. Predominant role of water in regulating soil and microbial respiration and their responses to climate change in a semiarid grassland. *Global Change Biology* 15: 184–195. https://doi.org/10.1111/j.1365-2486.2008.01728.x.

Livesley, S.J., and S.M. Andrusiak. 2012. Temperate mangrove and salt marsh sediments are a small methane and nitrous oxide source but important carbon store. *Estuarine Coastal and Shelf Science* 97: 19–27. https://doi.org/10.1016/j.ecss.2011.11.002.

Lohila, A., M. Aurela, K. Regina, and T. Laurila. 2003. Soil and total ecosystem respiration in agricultural fields: Effect of soil and crop type. *Plant and Soil* 251: 303–317.

Maljanen, M., J. Hytonen, P. Makiranta, J. Alm, K. Minkkinen, J. Laine, and P.J. Martikainen. 2007. Greenhouse gas emissions from cultivated and abandoned organic croplands in Finland. *Boreal Environment Research* 12: 133–140.

Megonigal, J.P., W.H. Patrick, and S.P. Faulkner. 1993. Wetland identification in seasonally flooded forest soils; soil morphology and redox dynamics. *Soil Science Society of America Journal* 57: 140–149.

Megonigal, J.P., M.E. Hines, and P.T. Visscher. 2004. Anaerobic metabolism: Linkages to trace gases and aerobic processes. In *Biogeochemistry*, ed. W.H. Schlesinger, 317–424. Oxford: Elsevier.

Mitsch, W.J., B. Bernal, A.M. Nahlik, Ü. Mander, L. Zhang, C.J. Anderson, S.E. Jørgensen, and H. Brix. 2013. Wetlands, carbon, and climate change. *Landscape Ecology* 28: 583–597. https://doi.org/10.1007/s10980-012-9758-8.

Myhre, G., D. Shindell, F.-M. Bréon, W. Collins, J. Fuglestvedt, J. Huang, D. Koch, J.-F. Lamarque, D. Lee, B. Mendoza, T. Nakajima, A. Robock, G. Stephens, T. Takemura, and H. Zhang. 2013. Anthropogenic and natural radiative forcing. In *Climate change 2013: The physical science basis; Working Group I contribution to the fifth assessment report of the Intergovernmental Panel on Climate Change*, ed. T. Stocker, 659–740. Cambridge: Cambridge University Press.

Nielsen, O.-K., M.S. Plejdrup, M. Winther, M. Nielsen, S. Gyldenkærne, M.H. Mikkelsen, R. Albrektsen, M. Thomsen, K. Hjelgaard, P. Fauser, H.G. Bruun, V.K. Johannsen, T. Nord-Larsen, L. Vesterdal, I. Stupak, N. Scott-Bentsen, E. Rasmussen, S.B. Petersen, T.M. Olsen, and M.G. Hansen. 2021. *Denmark's National Inventory Report 2021. Emission Inventories 1990–2019* - Submitted under the United Nations Framework Convention on Climate Change and the Kyoto Protocol. Aarhus University, DCE – Danish Centre for Environment and Energy, 944 pp. Scientific Report No. 437

Oppenheimer, M., B.C. Glavovic, J. Hinkel, R. van de Wal, A.K. Magnan, A. Abd-Elgawad, R. Cai, M. Cifuentes-Jara, R.M. DeConto, T. Ghosh, J. Hay, F. Isla, B. Marzeion, B. Meyssignac, and Z. Sebesvari. 2019. Sea level rise and implications for low-lying islands, coasts and communities. In: IPCC special report on the ocean and cryosphere in a changing climate [H.-O. Pörtner, D.C. Roberts, V. Masson-Delmotte, P. Zhai, M. Tignor, E. Poloczanska, K. Mintenbeck, A. Alegría, M. Nicolai, A. Okem, J. Petzold, B. Rama, N.M. Weyer (eds.)]. Cambridge University Press, Cambridge, UK and New York, NY, USA, pp. 321–445. https://doi.org/10.1017/9781009157964.006.

Pelletier, L., T.R. Moore, N.T. Roulet, M. Garneau, and V. Beaulieu-Audy. 2007. Methane fluxes from three peatlands in the La Grande Rivière watershed, James Bay lowland. *Canada. Journal of Geophysical Research* 112: G01018. https://doi.org/10.1029/2006JG000216.

Pendleton, L., D.C. Donato, B.C. Murray, S. Crooks, W.A. Jenkins, S. Sifleet, C. Craft, J.W. Fourqurean, J.B. Kauffman, N. Marbà, P. Megonigal, E. Pidgeon, D. Herr, D. Gordon, and A. Baldera. 2012. Estimating global "Blue Carbon" emissions from conversion and degradation of vegetated coastal ecosystems. *PLoS ONE* 7: e43542. https://doi.org/10.1371/journal.pone.0043542.

Pugh, C.A., D.E. Reed, A.R. Desai, and B.N. Sulman. 2018. Wetland flux controls: How does interacting water table levels and temperature influence carbon dioxide and methane fluxes in northern Wisconsin? *Biogeochemistry* 137: 15–25.

Reicosky, D.C., W.A. Dugas, and H.A. Torbert. 1997. Tillage-induced soil carbon dioxide loss from different cropping systems. *Soil & Tillage Research* 41: 105–118. https://doi.org/10.1016/s0167-1987(96)01080-x.

Sanches, L.F., B. Guenet, C.C. Marinho, N. Barros, and F. de Assis Esteves. 2019. Global regulation of methane emission from natural lakes. *Scientific Reports* 9: 255. https://doi.org/10.1038/s41598-018-36519-5.

Sanchez-Rodriguez, A.R., C.R. Nie, P.W. Hill, D.R. Chadwick, and D.L. Jones. 2019. Extreme flood events at higher temperatures exacerbate the loss of soil functionality and trace gas emissions in grassland. *Soil Biology & Biochemistry* 130: 227–236. https://doi.org/10.1016/j.soilbio.2018.12.021.

Schindler, T., Ü. Mander, K. Machacova, M. Espenberg, D. Krasnov, J. Escuer-Gatius, G. Veber, J. Pärn, and K. Soosaar. 2020. Short-term flooding increases CH4 and N2O emissions from trees in a riparian forest soil-stem continuum. *Scientific Reports* 10: 3204. https://doi.org/10.1038/s41598-020-60058-7.

Sha, C., W.J. Mitsch, U. Mander, J.J. Lu, J. Batson, L. Zhang, and W.S. He. 2011. Methane emissions from freshwater riverine wetlands. *Ecological Engineering* 37: 16–24. https://doi.org/10.1016/j.ecoleng.2010.07.022.

Sjøgaard, K.S., A.H. Treusch, and T.B. Valdemarsen. 2017. Carbon degradation in agricultural soils flooded with seawater after managed coastal realignment. *Biogeosciences* 14: 4375–4389. https://doi.org/10.5194/bg-14-4375-2017.

Skinner, C., A. Gattinger, A. Muller, P. Mader, A. Fliessbach, M. Stolze, R. Ruser, and U. Niggli. 2014. Greenhouse gas fluxes from agricultural soils under organic and non-organic management - a global meta-analysis. *Science of the Total Environment* 468: 553–563. https://doi.org/10.1016/j.scitotenv.2013.08.098.

Smith, K.A., T. Ball, F. Conen, K.E. Dobbie, J. Massheder, and A. Rey. 2018. Exchange of greenhouse gases between soil and atmosphere: Interactions of soil physical factors and biological processes. *European Journal of Soil Science* 69: 10–20. https://doi.org/10.1111/ejss.12539.

Smith, K.E., G.B. Runion, S.A. Prior, H.H. Rogers, and H.A. Torbert. 2010. Effects of elevated CO_2 and agricultural management on flux of greenhouse gases from soil. *Soil Science* 175: 349–356. https://doi.org/10.1097/SS.0b013e3181e93d3c.

Solomon, S., D. Qin, M. Manning, K. Averyt, and M. Marquis (Eds.). 2007. Climate change 2007-the physical science basis: Working group I contribution to the fourth assessment report of the IPCC (Vol. 4). Cambridge university press.

Soumis, N., E. Duchemin, R. Canuel, and M. Lucotte. 2004. Greenhouse gas emissions from reservoirs of the western United States. *Global Biogeochemical Cycles* 18: GB3022. https://doi.org/10.1029/2003GB002197.

Stenak, M. 2005. De inddæmmede landskaber – en historisk geografi (in Danish). Landbohistorisk selskab.

Tagesson, T., M. Mölder, M. Mastepanov, C. Sigsgaard, M.P. Tamstorf, M. Lund, J.M. Falk, A. Lindroth, T.R. Christensen, and L. Ström. 2012. Land-atmosphere exchange of methane from soil thawing to soil freezing in a high-Arctic wet tundra ecosystem. *Global Change Biology* 18: 1928–1940.

Taoka, T., H. Iwata, R. Hirata, Y. Takahashi, Y. Miyabara, and M. Itoh. 2020. Environmental controls of diffusive and ebullitive methane emissions at a subdaily time scale in the littoral zone of a midlatitude shallow lake. *Journal of Geophysical Research: Biogeosciences* 125: e2020JG005753.

Thorsen, S.W., M. Holmer, C.O. Quintana, T. Valdemarsen, and E. Kristensen. 2021. Internal nutrient loading controls macroalgal and cyanobacterial succession in a coastal lagoon restored by managed realignment of agricultural land. *Frontiers in Marine Science* 8: 649360.

Topp, E., and E. Pattey. 1997. Soils as sources and sinks for atmospheric methane. *Canadian Journal of Soil Science* 77: 167–178. https://doi.org/10.4141/s96-107.

Trumbore, S. 2006. Carbon respired by terrestrial ecosystems - recent progress and challenges. *Global Change Biology* 12: 141–153.

Turetsky, M.R., C.C. Treat, M.P. Waldrop, J.M. Waddington, J.W. Harden, and A.D. McGuire. 2008. Short-term response of methane fluxes and methanogen activity to water table and soil warming manipulations in an Alaskan peatland. *Journal of Geophysical Research* 113: G00A10. https://doi.org/10.1029/2007JG000496.

Valach, A.C., K. Kasak, K.S. Hemes, T.L. Anthony, I. Dronova, S. Taddeo, W.L. Silver, D. Szutu, J. Verfaillie, and D.D. Baldocchi. 2021. Productive wetlands restored for carbon sequestration quickly become net CO_2 sinks with site-level factors driving uptake variability. *PLoS ONE* 16: e0248398. https://doi.org/10.1371/journal.pone.0248398.

Von Fischer, J.C., G. Butters, P.C. Duchateau, R.J. Thelwell, and R. Siller. 2009. In situ measures of methanotroph activity in upland soils: A reaction-diffusion model and field observation of water stress. *Journal of Geophysical Research: Biogeosciences* 114: G01015. https://doi.org/10.1029/2008JG000731.

Vroom, R.J.E., M. van den Berg, S.R. Pangala, O.E. van der Scheer, and B.K. Sorrell. 2022. Physiological processes affecting methane transport by wetland vegetation – a review. *Aquatic Botany* 182: 103547. https://doi.org/10.1016/j.aquabot.2022.103547.

Wang, G.Q., X.H. Xia, S.D. Liu, L. Zhang, S.B. Zhang, J.F. Wang, N.N. Xi, and Q.R. Zhang. 2021. Intense methane ebullition from urban inland waters and its significant contribution to greenhouse gas emissions. *Water Research* 189: 116654. https://doi.org/10.1016/j.watres.2020.116654.

Welsh, M.K., P.G. Vidon, and S.K. McMillan. 2021. Riparian seasonal water quality and greenhouse gas dynamics following stream restoration. *Biogeochemistry* 156: 453–474.

Wik, M., P.M. Crill, R.K. Varner, and D. Bastviken. 2013. Multiyear measurements of ebullitive methane flux from three subarctic lakes. *Journal of Geophysical Research: Biogeosciences* 118: 1307–1321. https://doi.org/10.1002/jgrg.20103.

Wollenberg, J.T., A. Biswas, and G.L. Chmura. 2018. Greenhouse gas flux with reflooding of a drained salt marsh soil. *PeerJ* 6: e5659. https://doi.org/10.7717/peerj.5659.

Wu, S., S. Li, Z. Zou, T. Hu, Z. Hu, S. Liu, and J. Zou. 2019. High methane emissions largely attributed to ebullitive fluxes from a subtropical river draining a rice paddy watershed in China. *Environmental Science & Technology* 53: 3499–3507. https://doi.org/10.1021/acs.est.8b05286.

Yagi, K., and K. Minami. 1991. Emission and production of methane in the paddy fields of Japan. *JARQ: Japan Agricultural Research Quarterly* 25: 165–171.

Yvon-Durocher, G., A.P. Allen, D. Bastviken, R. Conrad, C. Gudasz, A. St-Pierre, N. Thanh-Duc, and P.A. del Giorgio. 2014. Methane fluxes show consistent temperature dependence across microbial to ecosystem scales. *Nature* 507: 488–491. https://doi.org/10.1038/nature13164.

Zhao, K., E.W. Tedford, and G.A. Lawrence. 2022. Ebullition regulated by pressure variations in a boreal pit lake. *Frontiers in Earth Science* 10: 850652. https://doi.org/10.3389/feart.2022.850652.